LOW-INTENSITY H-BETA EMISSION FROM THE INTERSTELLAR MEDIUM*

R. J. Reynolds, F. Roesler, and F. Scherb
Physics Department
University of Wisconsin
Madison, Wisconsin 53706

and

E. Boldt
Laboratory for High Energy Astrophysics
Goddard Space Flight Center
Greenbelt, Maryland 20771

Abstract

A search for diffuse galactic H-beta emission not associated with any known H II regions was conducted using a 2-inch diameter pressure-scanned Fabry-Perot spectrometer at the coudé focus of the 36-inch telescope at Goddard Space Flight Center.

Observations were made near the directions of four pulsars (PSR 0532, PSR 1508, PSR 1541 and PSR 1642) between November 1969 and June 1970. Emissions with intensities from 4×10^4 to 40×10^4 photons/cm^2 sec ster (corresponding to emission measures of approximately 10 - 100) were detected in three of the directions. The data indicate an average ionization rate (assuming steady state) of $\simeq 10^{-14}$ /H-atom sec for the interstellar hydrogen in these directions and temperatures between 10^3 °K and 10^4 °K for the emitting regions.

Plans have been made to continue the investigation of these very faint hydrogen emission sources using a 6-inch diameter Fabry-Perot spectrometer.

* Supported in part by National Aeronautics and Space Administration grants No. NGL 50-002-044 and No. 50-002-162, and by the University of Wisconsin Graduate School.

Introduction

Before the discovery of pulsars, the state of ionization in H I regions was generally attributed to the ionizing effect of starlight on elements whose ionization potentials are smaller than that of hydrogen. For example, ultraviolet radiation escapes from H II regions surrounding hot stars and can produce ions such as C^+, Si^+, and Fe^+ in H I regions. From the known abundances of these elements in the Galaxy, this model for the ionization state in H I regions leads to an electron density n_e given by

$$n_e/n_H \simeq 5 \times 10^{-4}, \tag{1}$$

where n_H is the neutral hydrogen density.

Since the discovery of pulsars, observations of pulse dispersions give direct information on electron densities in the interstellar medium. In particular these observations determine the dispersion measure d.m. given by

$$\text{d.m.} = \int_0^d n_e \, ds, \tag{2}$$

where d is the distance to the pulsar. In addition, observations of the 21-cm line of atomic hydrogen can determine the columnar density N_H of neutral hydrogen in the Galaxy, given by

$$N_H = \int n_H \, ds. \tag{3}$$

Some idea of the order of magnitude of the quantity n_e/n_H can be obtained from the ratio of d.m. to N_H. Values of $\text{d.m.}/N_H \simeq 0.05$ are typical, implying electron densities roughly 100 times larger than expected from ionization by starlight. Therefore, either the number densities of C^+, Si^+, and Fe^+ are 100 times larger than the generally assumed values or additional ionization processes occur which also ionize hydrogen.

Ionization of the interstellar hydrogen, whatever the mechanism, leads to the emission of recombination radiation. In general the intensity of a particular hydrogen line is given by

$$I_y = \frac{1}{4\pi} \int \epsilon_y \, \alpha(T_e) \, n_e \, n_{H^+} \, e^{-\tau_y(s)} \, ds, \tag{4}$$

where y denotes a particular recombination line, ϵ_y is the probability of a y-photon being emitted per recombination, T_e is the electron temperature, $\alpha(T_e)$ is the effective recombination coefficient, n_{H^+} is the proton density, and $\tau_y(s)$ is the optical depth to y-photons of a point at a distance s. Assuming a steady state, I_y is also given by

$$I_y = \frac{1}{4\pi} \int \epsilon_y \, \zeta \, n_H \, e^{-\tau_y(s)} \, ds, \tag{5}$$

where ζ is the ionization rate per hydrogen atom. It can be shown that ϵ_y varies slowly with T_e. For H-beta, $\epsilon_{H\beta}$ has a nearly constant value of 0.12 for $10^2 < T_e < 10^5$ °K. Therefore, if ζ is assumed to be constant throughout the interstellar medium, ζ is given by

$$\zeta = \frac{4\pi}{\epsilon_{H\beta}} \cdot \frac{I_{H\beta}}{\int n_H \, e^{-\tau_{H\beta}} \, ds} \tag{6}$$

In directions of low 21-cm absorption, e.g., in high galactic latitudes, the columnar density of neutral hydrogen can be directly determined from 21-cm emission measurements. Assuming small optical absorption in these directions, measurements of $I_{H\beta}$ result in a direct determination of ζ, given by

$$\zeta = 105 \frac{I_{H\beta}}{N_H}, \tag{7}$$

where $I_{H\beta}$ is in units of cm^{-2} sec^{-1} $ster^{-1}$ and N_H is in units of cm^{-2}. If the value of ζ is not assumed to be a constant along the line of sight, the $I_{H\beta}$ determines an average ionization rate $\langle \zeta \rangle$.

In addition, measurements of $I_{H\beta}$ and a knowledge of the temperature can be combined with pulsar dispersion measures to determine various parameters of

the interstellar medium including limits on the electron densities and sizes of the emitting regions. In directions of little reddening or where the reddening is accurately known, the emission measure e.m., defined by

$$\text{e. m.} = \int n_e^2 \, ds \tag{8}$$

can be computed from $I_{H\beta}$ and T_e using values for the H_β emissivity of hydrogen computed by Pengelly (1963). The values of e.m. and d.m. can then be used to set limits on both the total length L along the line of sight occupied by the emitting regions and on the average electron density $\langle n_e \rangle$ within these regions, defined by

$$\langle n_e \rangle = N_e / L, \tag{9}$$

where N_e, the columnar electron density through the galactic disk, is defined by

$$N_e = \int n_e \, ds. \tag{10}$$

(Assuming the pulsars are confined to the galactic disk, d.m. must always be a lower limit to N_e.) The mean square deviation, $\Delta^2 n_e$, of n_e from $\langle n_e \rangle$ along the line of sight within these regions is defined by the relation

$$\Delta^2 n_e = \frac{1}{L} \int (n_e^2 - \langle n_e \rangle^2) \, ds. \tag{11}$$

From this relation and the definition (9) of $\langle n_e \rangle$ it follows that

$$\langle n_e \rangle = \frac{1}{\left[1 + \dfrac{\Delta^2 n_e}{\langle n_e \rangle^2}\right]} \cdot \frac{\text{e.m.}}{N_e}, \tag{12}$$

and

$$L = \left[1 + \frac{\Delta^2 n_e}{\langle n_e \rangle^2}\right] \frac{N_e^2}{e.m.} \cdot \tag{13}$$

Since

$$N_e \geq d.m., \tag{14}$$

and

$$\frac{\Delta^2 n_e}{\langle n_e \rangle^2} \geq 0, \tag{15}$$

the limits on $\langle n \rangle_e$ and L are given by

$$\langle n_e \rangle \leq e.m./d.m. \tag{16}$$

and

$$L \geq \frac{(d.m.)^2}{e.m.} \cdot \tag{17}$$

For regions having an approximately uniform electron distribution

$$\left(\frac{\Delta^2 n_e}{\langle n_e \rangle^2} << 1\right),$$

and in a direction where the pulsar dispersion measure is approximately the total columnar electron density (d.m. $\simeq N_e$), the computed limits given by (16) and (17) would be close to the actual values of $\langle n_e \rangle$ and L. A comparison of $(d.m.)^2/e.m.$ with the total distance through the galactic disk in that direction would then be a measure of the "clumpiness" of these regions within the interstellar medium.

Assuming a steady-state ionization process, the intensity of H-beta from the H I interstellar medium can be estimated.* For X-ray or cosmic ray ionization,

* The expected intensities of various radiations resulting from cosmic ray ionization and heating have been calculated in detail by Hayakawa et al. (1960) and Balasubrahmanyan et al. (1967).

the ionization rate ζ for equilibrium models has been estimated as 10^{-15} /H atom sec (Field et al. 1969, Werner et al. 1970, Hjellming et al. 1969). Therefore, for an H I cloud occupying 20 pc along the line of sight with a density of 20 hydrogen atoms/cm^3 ($N_H = 12.3 \times 10^{20}$/cm^2) at a distance s from the earth such that $\tau_{H\beta} << 1$ ($\tau_{H\beta} \simeq 1$ for s = 1 kpc in the galactic plane), equation (5) gives

$$I_{H\beta}^{cloud} = 1 \times 10^4/cm^2 \text{ sec ster.} \tag{18}$$

The intensity from the intercloud medium in the plane of the galaxy is estimated by integrating over one absorption mean free path for H-beta (1 kpc). Assuming that $n_H = 1.0$ cm^{-3} ($N_H = 31 \times 10^{20}$/cm^2),

$$I_{H\beta}^{intercloud} = 3 \times 10^4/cm^2 \text{ sec ster.} \tag{19}$$

The H-beta emission from a "classical" H II region is normally the result of ionization due to ultraviolet radiation from nearby O and B stars. Assuming a diameter of 20 pc and $n_e = 3 - 10$ cm^{-3}, then

$$I_{H\beta}^{H\,II} = 10^6 - 10^7/cm^2 \text{ sec ster.} \tag{20}$$

In general, the hydrogen emission from a particular direction could include radiation from all these sources: H II regions, H I clouds, and the intercloud medium. With a spectrometer of sufficient sensitivity and resolving power these sources may be distinguished from one another. For example the position and shape of the H-beta emission profiles could be compared with the position and shape of 21-cm features. Such a comparison should then help determine whether the H-beta emissions were originating from H I regions. Also it could be possible to distinguish these three sources from one another on the basis of the measured widths of the emission lines and the intensity ratio $I_{H\alpha}/I_{H\beta}$. For example, a cloud at a temperature of about 100°K would emit H-beta with a characteristic line width $\Delta\lambda \simeq 0.03$Å and $I_{H\alpha}/I_{H\beta} \simeq 8$, whereas for an H II region at 10 °K, $\Delta\lambda \simeq 0.34$Å and $I_{H\alpha}/I_{H\beta} \simeq 4$. (Actually these line widths $\Delta\lambda$ are the widths of the two fine structure components of the H-beta line, which are separated by 0.078Å).

The results of the preceding discussion are summarized in Table 1.

Table 1

H-beta Source	T_e (°K)	n_H (cm^{-3})	n_e (cm^{-3})	N_H ($\times 10^{20}$ cm^{-2})	$I_{H\beta}$ $\left(\frac{\text{photons}}{cm^2 \text{ sec ster}}\right)$	$\Delta\lambda$ (Å)	$\frac{I_{H\alpha}}{I_{H\beta}}$
H I cloud	10^2	20	0.050	12	1×10^4	0.03	8
Intercloud medium	10^3	1.0	0.025	31	3×10^4	0.10	5
H II region	10^4	~0	3-10	~0	10^6 - 10^7	0.34	4

Faint H-beta emissions that did not appear to be associated with any known H II regions have been observed by Johnson (1970) using wide-band filters and by Hindle et al. (1967), Daehler et al. (1968), and Reay and Ring (1969) using relatively low resolution (0.6Å) Fabry-Perot spectrometers. Because of the low resolution they could not accurately discriminate between galactic and local emissions, nor could they measure the line profiles of the emission.

A search for faint galactic H-beta emission with relatively high resolution (0.13Å) was conducted using a 2-inch diameter pressure-scanned Fabry-Perot etalon at the coudé focus of the 36-inch telescope at Goddard Space Flight Center. The observations were conducted between October, 1969 and June, 1970.

Instrumentation

The Fabry-Perot etalon as a spectrometer has been discussed widely in the literature (Mack et al. 1963, Roesler 1967, Jacquinot 1954). In general a spectrometer can be characterized by two quantities: the resolving power R, and the luminosity L, which is proportional to the flux transmitted by the spectrometer. The fact that the product LR of a Fabry-Perot etalon can be made much greater (30 to 400 times) than that for a prism or grating of equal area (Jacquinot 1954) makes the Fabry-Perot spectrometer particularly well suited for observations of emission lines from faint extended sources, i.e., for a given resolution, the light can be collected over a relatively large solid angle.

Figure 1 illustrates the combined transmission curve of an etalon and 6Å FWHM interferences filter used in the observations. The filter was necessary to suppress all etalon transmission peaks except those near the wavelength of interest.

Observations

The H-beta recombination line was chosen because its wavelength is near the peak of the S20 photocathode response curve and because the local sky background is low in this wavelength region relative to H-alpha (Eather 1969). Although observations of both the H-beta and H-alpha fluxes are desirable, as will soon be evident, the combination of weak line intensity, low instrumental quantum efficiency, and the limited time available did not permit the study of both H-beta and H-alpha emissions.

In order to maximize the signal-to-noise ratio, in addition to using optical coatings and a cooled photocathode, virtually all observations were restricted to moonless nights with low atmospheric extinction, and, using the 6-inch finder telescope, care was taken to eliminate any stars brighter than 11th magnitude from the 1.5 arc minute field of view. The various contributions to the photomultiplier count rate on a clear, moonless night in and out of the galactic plane are given in Table 2. The signal count rate has been normalized to 0.1/sec and represents the rate at the peak of the line. Such a rate roughly corresponds to the intensities observed.

Table 2

Contributions to Total Count Rate

Source	in galactic plane	out of galactic plane
dark count	0.6/sec	0.6/sec
sky background	1.0/sec	0.4/sec
emission line	0.1/sec	0.1/sec
total	1.7/sec	1.1/sec
signal/noise	0.08	0.10

Regions near the pulsars PSR 0532 (Crab Nebula pulsar), PSR 1508, PSR 1541, and PSR 1641 were studied. The bulk of the observations in the direction near the Crab were made in January and February, 1970, while those in the directions of the other three pulsars were made in the interval from May 29 through June 7, 1970.

It was assumed that the emission would be approximately centered about the local standard of rest (LSR) velocity because by definition this is the velocity about which the local intercloud medium and the individual H I clouds are

expected to be centered on the average. Since the Crab is close to the galactic anticenter direction ($\ell^{II} = 182°$, $b^{II} = -6°$), there are no galactic rotation effects in this direction, and all the material along the line of sight should have velocities centered about the LSR velocity. Figures 2 and 3 give 21-cm data for the four regions studied and show that the assumption is justified.

The observations near PSR 0532 were made on a 1.5 arc minute diameter region (the field of view of the spectrometer) located approximately 9 arc minutes from the center of the Crab. The observational results in this direction are presented in Figure 4 where the accumulated counts are plotted as a function of wavelength (and velocity). The data were obtained by two different procedures. In the top two graphs, Figures 4a and 4b, the points represent the count rates at discrete wavelength positions near the LSR wavelength of H-beta. The bottom graph, Figure 4c, represents the result of an attempt to measure the line profile of the emission. It is the summation of 62 individual continuous pressure scans taken between November 15, 1969 and February 28, 1970. Each point represents an accumulation time of 3720 seconds over a wavelength interval of 0.066Å.

There is little doubt that the data in Figure 4 represent real emission, but to establish that the emission was galactic H-beta requires some additional discussion. Because a single etalon produces an ambiguity in the position of a line, the emission could have been an atmospheric line at any one of the permitted wavelengths: $\lambda_{LSR} \pm 1.23k$Å, where k = 0, 1, 2, 3, . . . However, observations were also made in another direction at the same wavelengths at which the emission was observed from the Crab direction and no emission was detected. Therefore, it appears unlikely that the emission was an atmospheric line. The emission also could not have been H-beta from the geocorona or solar system, since all the data were obtained when the LSR velocity for the Crab direction was about 35 km/sec (0.6Å) to either side of the H-beta rest wavelength. Any emission at the rest wavelength of H-beta would have appeared as a flat background since it would have been just half-way between two transmission peaks of the etalon. Also any emission at rest with respect to the sun would have been centered about 11 km/sec (0.2Å) to the blue of the observed emission.

During the observing period from May 30 through June 7, 1970, observations were made in the directions of PSR 1508 ($\ell^{II} = 91°$, $b^{II} = +50°$), PSR 1541 ($\ell^{II} = 18°$, $b^{II} = +46°$) and PSR 1642 ($\ell^{II} = 14°$, $b^{II} = +26°$). The resulting data are shown in Figures 5, 6, and 7. Although the statistics are poor, emissions appear to be present at the LSR velocities in the first two directions. There is some ambiguity as to whether the emissions from the PSR 1508 and PSR 1541 directions are galactic or local since the rest and LSR velocities in these two cases are separated by an amount equal to or less than the resolution of the spectrometer ($\simeq$ 8 km/sec). However, the expected flux of H-beta photons from

the geocorona is much too low to have contributed significantly to the observed flux. Meier (1969) estimates the H-alpha intensity from the geocoronal absorption of solar Lyman-beta in directions greater than 90° from the Sun to be less than $4 \times 10^5/cm^2$ sec ster. Therefore, from the ratio of fluxes of solar Lyman-beta to Lyman-gamma (Hinteregger 1961), and using the values for the absorption cross sections of these two lines and the branching ratios from the n = 3 and n = 4 levels given by Allen (1955) and Bethe and Salpeter (1957), we have

$$I_{H\beta}^{\text{geocorona}} < 5.5 \times 10^3/cm^2 \text{ sec ster}, \tag{21}$$

which is (as will be seen) about one order of magnitude below the observed intensities. The possibility that the observed emissions were due to the absorption of solar Lyman-gamma by a much larger amount of hydrogen perhaps within the solar system cannot be excluded.

In the direction near PSR 1642 no emission was detected at the LSR wavelength.

Because of the rather poor statistics, the widths of the emission lines could not be accurately measured. Therefore, $I_{H\beta}$ and the quantities that can be derived from $I_{H\beta}$ ($<\zeta>$, e.m., and limits on $<n_e>$ and L) can only be determined as functions of the assumed temperature and turbulent velocities within the emitting regions.

Tables 3 and 4 list these quantities computed from the observed emission near the Crab direction and from the extinction in this region as given by O'Dell (1960). In Table 3 the emission was assumed to be originating from regions occupying a total distance L along the line of sight and distributed uniformly out to the distance of the Crab. The rms random velocity V_{rms} of these regions (or the combination of random velocities and internal turbulent motions) was assumed to be 10 km/sec. The quantity α is the fraction of the line of sight distance occupied by the emission regions. In Table 3, α was computed from the relation

$$\alpha = \frac{L}{2000} \geq \frac{(\text{d.m.})^2/\text{e.m.}}{2000}. \tag{22}$$

In Table 4, the emission was assumed to be originating from a region centered on the Crab at a distance of 2 kpc. Attributing the observed value of d.m. to such a region implies that the value of the columnar electron density N_e used in the calculations was given by $n_e = 2\text{d.m.}$

Table 3

PSR 0532

d.m. = 56 cm^{-3} pc; V_{rms} = 10 km/sec

T_e (°K)	$I_{H\beta} \times 10^{-4}$ ($cm^{-2} sec^{-1} ster^{-1}$)	e.m. (cm^{-6} pc)	$\langle n_e \rangle$ (cm^{-3})	L (pc)	α
100	16	2.8	≤ 0.050	≥ 1100	≥ 0.55
1000	18	11	≤ 0.19	≥ 300	≥ 0.15
10000	39	130	≤ 2.3	≥ 24	≥ 0.01

Table 4

Emitting Region Centered on PSR 0532

V_{rms} = 0 km/sec

T_e (°K)	$I_{H\beta} \times 10^{-4}$ ($cm^{-2} sec^{-1} ster^{-1}$)	e.m. (cm^{-6} pc)	$\langle n_e \rangle$ (cm^{-3})	L (pc)	α
100	12	7.1	≤ 0.063	≥ 1800	≥ 0.90
1000	14	28	≤ 0.25	≥ 440	≥ 0.22
10000	32	371	≤ 3.3	≥ 34	≥ 0.02

Tables 5, 6, and 7 list the parameters for the directions near PSR 1508, PSR 1541, and PSR 1642 respectively. Because of the high galactic latitudes of these pulsars, extinction was neglected in the calculations. The values of α were computed from the relation,

$$\alpha = L \frac{\sin b^{II}}{H} \geq \frac{(d.m.)^2}{e.m.} \cdot \frac{\sin b^{II}}{H} \qquad (23)$$

where H, the half-thickness of the galaxy, was assumed to be 200 pc and b^{II} is the galactic latitude of the direction of the observation. Since in the PSR 1642 direction only an upper limit to the peak count rate could be determined, the

Table 5

PSR 1508

d.m. = 19.6 cm^{-3} pc; V_{rms} = 10 km/sec

T_e (°K)	$I_{H\beta} \times 10^{-4}$ ($cm^{-2} sec^{-1} ster^{-1}$)	e.m. (cm^{-6} pc)	$\langle n_e \rangle$ (cm^{-3})	L (pc)	α
100	4.0	0.28	≤ 0.014	≥ 1400	–
1000	4.5	1.1	≤ 0.055	≥ 360	–
10000	9.0	12	≤ 0.62	≥ 32	≥ 0.13

Table 6

PSR 1541

d.m. = 35 cm^{-3} pc; V_{rms} = 10 km/sec

T_e (°K)	$I_{H\beta} \times 10^{-4}$ ($cm^{-2} sec^{-1} ster^{-1}$)	e.m. (cm^{-6} pc)	$\langle n_e \rangle$ (cm^{-3})	L (pc)	α
100	11	0.79	≤ 0.023	≥ 1600	–
1000	12	3.0	≤ 0.085	≥ 410	–
10000	20	26	≤ 0.75	≥ 47	≥ 0.17

Table 7

PSR 1642

d.m. = 40 cm^{-3} pc; V_{rms} = 10 km/sec

T_e (°K)	$I_{H\beta} \times 10^{4}$ ($cm^{-2} sec^{-1} ster^{-1}$)	e.m. (cm^{-6} pc)	$\langle n_e \rangle$ (cm^{-3})	L (pc)	α
100	≤ 3.4	≤ 0.24	≤ 0.006	≥ 6700	–
1000	≤ 3.7	≤ 0.89	≤ 0.022	≥ 1800	–
10000	≤ 7.5	≤ 10	≤ 0.25	≥ 160	≥ 0.35

values computed for $I_{H\beta}$ and e.m. are upper limits with a 90% confidence limit at each temperature.

The data presented in the tables imply that the observed emission could have originated from any one of a variety of possible regions. For example, the data in Table 3 suggest that the emission may have been either regions occupying approximately 15 percent of the line-of-sight distance with $T_e \cong 10^3$ °K and $n_e \cong 0.19$ cm^{-3} or from a tenuous H II region about 24 pc in diameter with $n_e \cong 2$ cm^{-3} and $T_e \cong 10^4$ °K.

There are some further statements that can be made about the interstellar medium using the data that were obtained. First, a lower limit can be placed on the average ionization rate $<\zeta>$ along the line of sight, given by Eq. (7). Columnar hydrogen densities N_H in the directions of pulsars are given by Davies (1969) and a more recent compilation of values of N_H has been made by Daltabuit (1970). For each direction the lower limit to $<\zeta>$ was computed by choosing the largest value of N_H from the two compilations and the lowest possible value for $I_{H\beta}$. This latter limit corresponds to assuming a continuous, uniform emitting region ($T_e < 10^3$ °K) along the total line of sight distance through the galaxy. In the direction of PSR 1642 it was not possible to place a lower limit on $<\zeta>$ since no emission was observed.

Secondly, lower limits can be set on the temperatures in the directions of PSR 1508, PSR 1541, and PSR 1642. Since the path lengths through the galactic disk in these directions are less than 300 or 400 pc, the data in Tables 5, 6, and 7 suggest that the temperatures of the emitting regions are greater than 10^3 °K. From the line profile obtained in the Crab direction an upper limit on the temperature can be placed in that direction:

$$T \leq 2 \times 10^4 \text{ °K (90\% confidence interval)}$$

$$T \leq 1 \times 10^4 \text{ °K (60\% confidence interval)}$$

More restrictive limits on the temperatures can be obtained from the radio absorption measurements of Ellis and Hamilton (1966). By assuming that the absorption of the galactic radio radiation below 20 MHz is caused by free-free transitions of ionized hydrogen, they were able to compute as a function of galactic latitude a quantity they call the absorption index a.i. defined by

$$\text{a.i.} = \int \frac{n_e^2}{(T/10^4)^{3/2}} \, \text{d.s.} \tag{24}$$

Table 8

Limits On $\langle\zeta\rangle$

Direction	$I_{H\beta}$ Minimum ($\times 10^{-2}$ /cm^{2}sec ster)	N_H Maximum ($\times 10^{20}$ cm^{-2})	$\langle\zeta\rangle$ Minimum ($\times 10^{-15}$/sec atom)
PSR 0532	16 ± 4	43†	9.5 ± 2.4
PSR 1508	4.0 ± 1.6	4.9†	8.6 ± 3.5
PSR 1541	11 ± 5	8.0*	14 ± 7

† Davis (1969)
* Daltabuit (1970)

They found that a.i. varied smoothly* with galactic latitude in a way consistent with a uniform disk-like distribution of ionized hydrogen. The values for a.i. were computed for southern galactic latitudes, but, assuming galactic symmetry about the solar position†, values for a.i. could be estimated in the directions of the H-beta observations. If uniform temperatures are assumed in the regions occupied by the electrons, the emission measure can be written as

$$\text{e.m.} = \text{a.i.}\ (T/10^4)^{3/2}. \tag{25}$$

Since these values for e.m. determined by radio absorption techniques have a different functional dependence on temperature than the values determined by observations of H-beta recombination lines, a graphical comparison of both data as shown in Figure 8 can be used to determine the temperatures which are compatible with both types of observations in a particular direction. These temperatures together with the temperature limits determined from previous considerations are summarized in Table 9. Depending upon the particular direction, temperatures from 1,600 °K to 11,000 °K are indicated for the emitting regions.

Referring back to Tables 3, 5, 6, and 7, the higher temperatures that are indicated by the comparisons with radio data suggest that the emission regions have electron densities (depending upon the particular direction) in the range 0.1 to 2.5 cm^{-3} and occupy anywhere from 1% to 100% of the line of sight distance through the galactic plane.

---

* The beamwidth of the radiotelescope was ~ 8 °.
† Rocket observations of the north galactic pole by Alexander and Stone (1965) are consistent with this assumption.

Table 9

Limits on Emission Region Temperatures

Direction	b^{II} (deg)	T(°K)		
		from line profile	from condition $\alpha \leq 1.0$	from comparison of Hβ and radio
PSR 0532	- 6	$<10^4$	–	1.6×10^3 to 1.1×10^4
PSR 1508	+52	–	$\gtrsim 1.4 \times 10^3$	2.5×10^3
PSR 1541	+46	–	$\gtrsim 1.6 \times 10^3$	1.0×10^4
PSR 1642	+26	–	$\gtrsim 4.3 \times 10^3$	1.6×10^3

Discussion

According to a model by Bottcher et al. (1970), large sections of the interstellar medium are ionized by ultraviolet photons from supernova explosions (Morrison and Sartori 1969). Such an effect could also arise from highly ionizing subrelativistic nuclei (e.g.: Si and Fe) ejected by these explosions (Ramaty et al. 1971). Since the cooling time for the medium is much shorter than the recombination time, the medium quickly cools after a supernova occurs, leaving behind a high residual amount of ionization. Therefore, along a given line of sight, various regions of the interstellar gas are in different stages of relaxation depending upon when the last supernova in each particular region occurred. The H-beta data at high galactic latitudes are consistent with this model, assuming that a sufficient time has elapsed (since the occurrence of supernovae in those directions) to have allowed the regions to cool from an initial 10^5 °K (Cox 1970) down to $\sim 10^4$ °K. But in the vicinity of the Crab Nebula, since the Crab supernova occurred only 10^3 years ago, the hydrogen still should be nearly 100 per cent ionized and at a temperature near 8×10^4 °K (Lenzen and Cox 1970). Using a value of 10^{61} photons/outburst and an interstellar hydrogen density of 1 cm^{-3}, the diameter of this region would be about 100 pc corresponding to a region on the sky 3° in diameter. The associated H-beta intensity from this region at the Earth would be 1.1×10^4 cm^{-2} sec^{-1} $sterad^{-1}$ in a line 1 Å wide. The observed emission in the direction of the Crab, therefore, cannot be explained by such a model. This does not eliminate the possibility, however, that some or most of the dispersion measure may be due to such a region. This would have the effect of leaving fewer electrons available to produce the observed emission, thus increasing the limits on $<n_e>$ and decreasing the limits on L in Table 4, for example.

These investigations will be continued at the Goddard telescope, using a 6-inch diameter etalon system which has 10 times the collecting area of the 2-inch system. It should be remembered that the line intensities that have been observed correspond to emission measures as low as 10 for temperatures of 10^4 °K and emission measures less than one for temperatures as low as 100 °K. Therefore, it is hoped that the 6-inch system will be a powerful tool in the search for and investigation of extended emission sources which are too faint to have been observed by other methods.

Acknowledgements

It is a pleasure to thank Dr. V. K. Balasubrahmanyan for anticipating the value of the measurements and Dr. Pierre Connes for suggesting the use of a pressure-scanned Fabry-Perot spectrometer.

References

Alexander, J. K., and Stone, R. G. 1965, Ap. J., 142, 1327.

Allen, C. W. 1955, Astrophysical Quantities (London: The Athlone Press).

Balasubrahmanyan, V. K., Boldt, E., Palmeira, R. A. R., and Sandri, G. 1967, G.S.F.C. Report X-611-67-357.

Bethe, H. A., and Salpeter, E. E. 1957, Quantum Mechanics of One- and Two-Electron Atoms (New York: Academic Press).

Bottcher, C., McCray, R. A., and Dalgarno, A. 1970, Astrophys. Lett., 6, 237.

Cox, D. P. 1970, private communication.

Daehler, M., Mack, J. E., Stoner, Jr., J. O., Clark, D., and Ring, J. 1968, Planet. Space Sci., 16, 795.

Daltabuit, E. 1970, private communication.

Davies, R. D. 1969, Nature, 223, 355.

Eather, R. 1969, private communication.

Ellis, G. R. A., and Hamilton, P. A. 1966, Ap. J., 146, 78.

Field, G. B., Goldsmith, D. W., and Habing, J. J. 1969, Ap. J., 155, L149.

Hayakawa, S., Nishimura, S., and Takayanagi, K. 1961, Pub. Astr. Soc. Japan, 13, 184.

Hindle, P. H., Reay, N. K., and Ring, J. 1968, Planet. Space Sci., 16, 803.

Hinteregger, H. E. 1961, J. Geophys. Res., 66, 2367.

Hjellming, R. M., Gordon, C. P., and Gordon, K. J. 1969, Astron. and Astrophys., 2, 202.

Jacquinot, P. 1954, J. Opt. Soc. Amer., 44, 761.

Johnson, H. M. 1970, preprint.

Lenzen, A., and Cox, D. P. 1970, private communication.

Mack, J. E. et al. 1963, Applied Optics, 2, 873.

Meier, R. R. 1969, J. Geophys. Res., 74, 3561.

Morrison, P., and Sartori, L. 1969, Ap. J., 158, 541.

Müller, C. A. 1959, Paris Symposium on Radio Astronomy, ed. R. N. Bracewell (Stanford: Stanford University Press), p. 360.

O'Dell, C. R. 1962, Ap. J., 136, 809.

Pengelly, R. M. 1963, M.N.R.A.S., 127, 145.

Reay, N. K., and Ring, J. 1969, Planet. Space Sci., 17, 561.

Roesler, F. L., and Mack, J. E. 1967, Journal de Physique, C2, 313.

Tolbert, C. R. and Fejes, I. 1969, preprint.

Werner, W. W., Silk, J., and Rees, M. J. 1970, Ap. J., 161, 965.

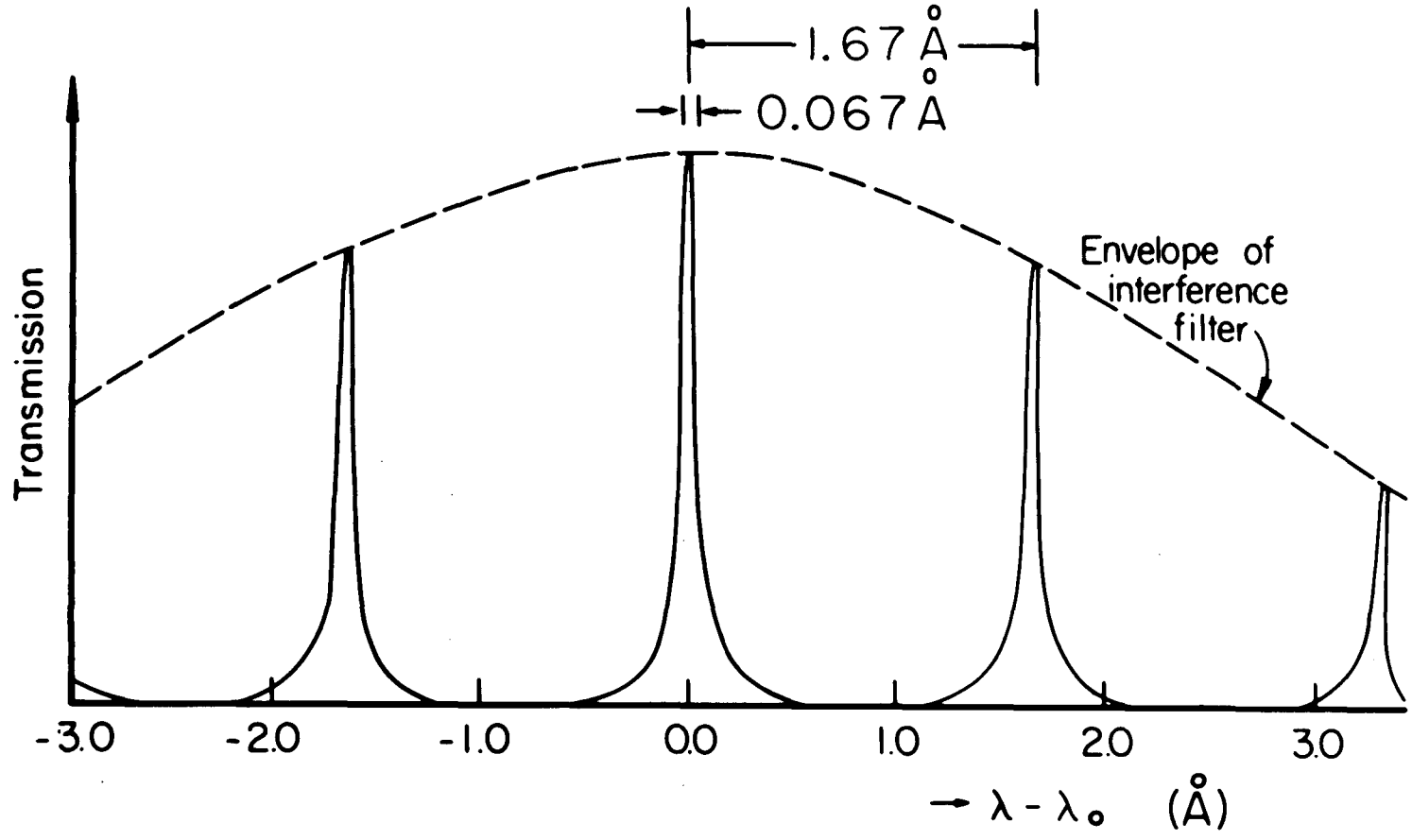

Figure 1. Transmission of etalon for small apertures in series with a 6 Å interference filter centered on wavelength $\lambda_0 = 4861$ Å.

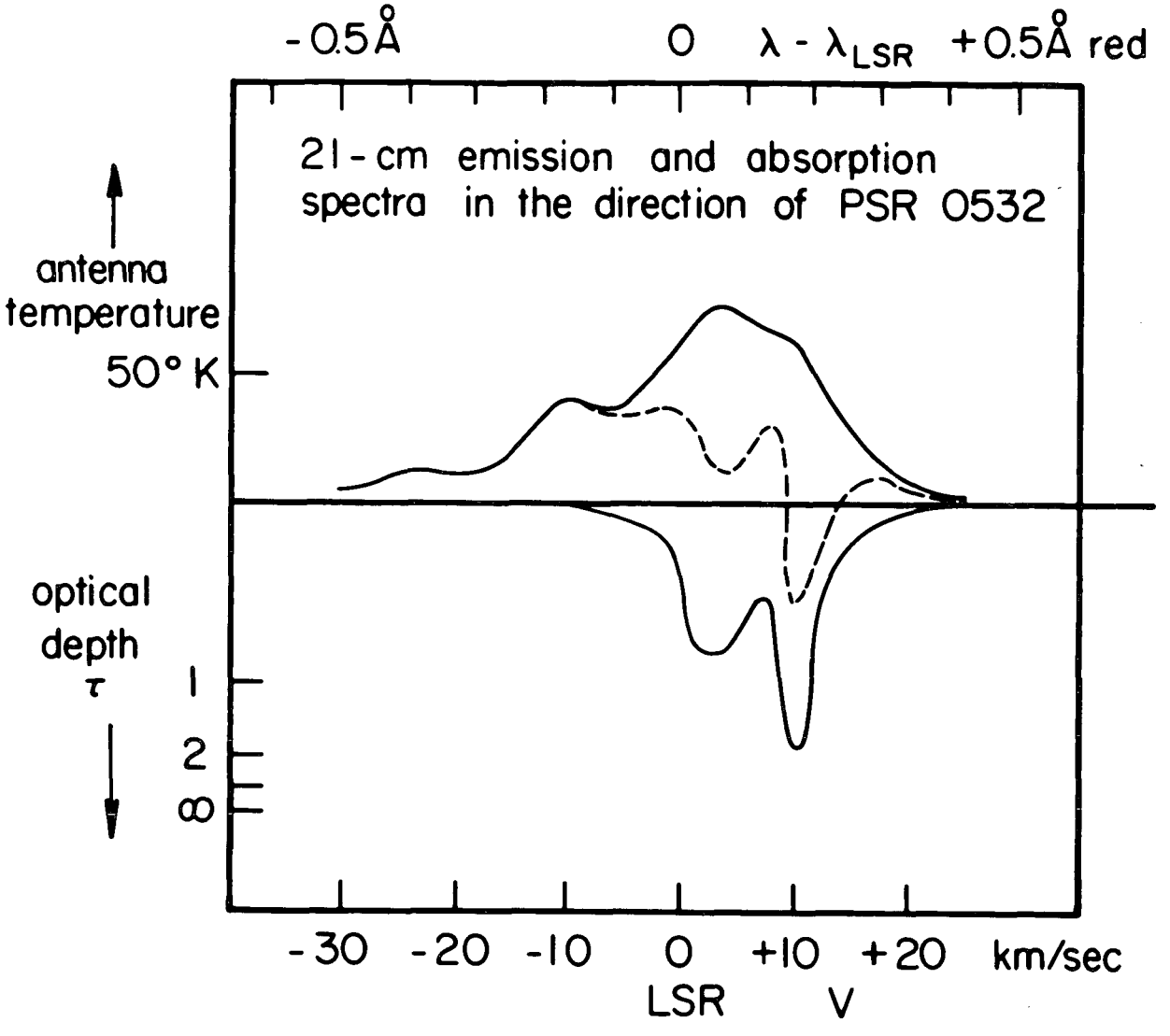

Figure 2. 21-cm emission and absorption spectra in the direction of PSR 0532 as given by Müller (1959). The dashed curve represents the observed profile from which are derived:

upper curve: the expected emission profile

lower curve: the expected absorption profile.

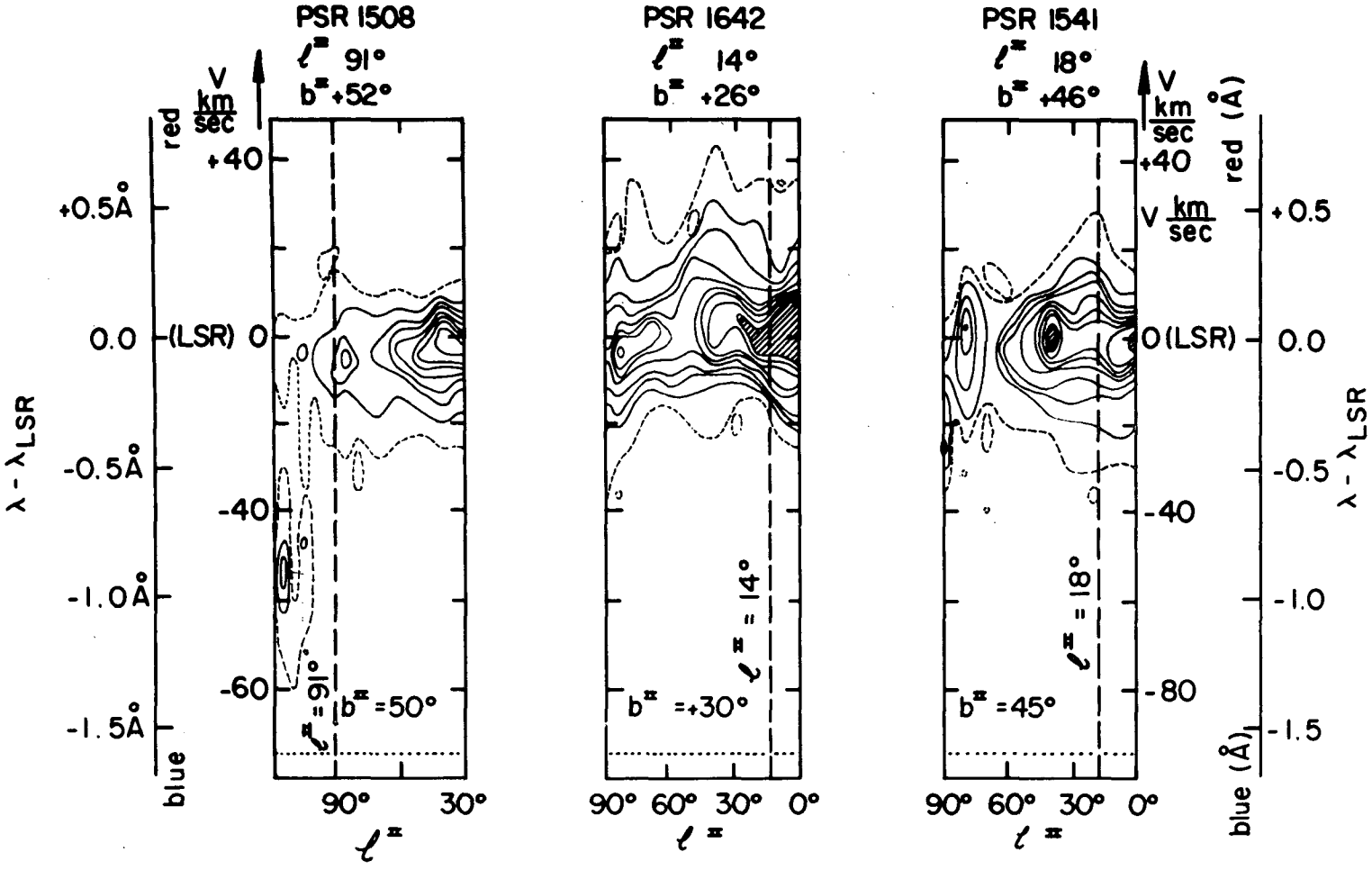

Figure 3. 21-cm emission data as given by Tolbert and Fejes (1969):

a) near direction of PSR 1508

b) near direction of PSR 1642

c) near direction of PSR 1541.

The contour values, indicated by varying line thickness, are 1 (dashed line), 2, 3, 4, 6, 8, 10, and 14 units, where 1 unit equals ≃1°K in brightness temperature. All intensities greater than 18 units are shaded. Note that the 21-cm emission is centered on the LSR (0 km/sec) velocity in all three directions.

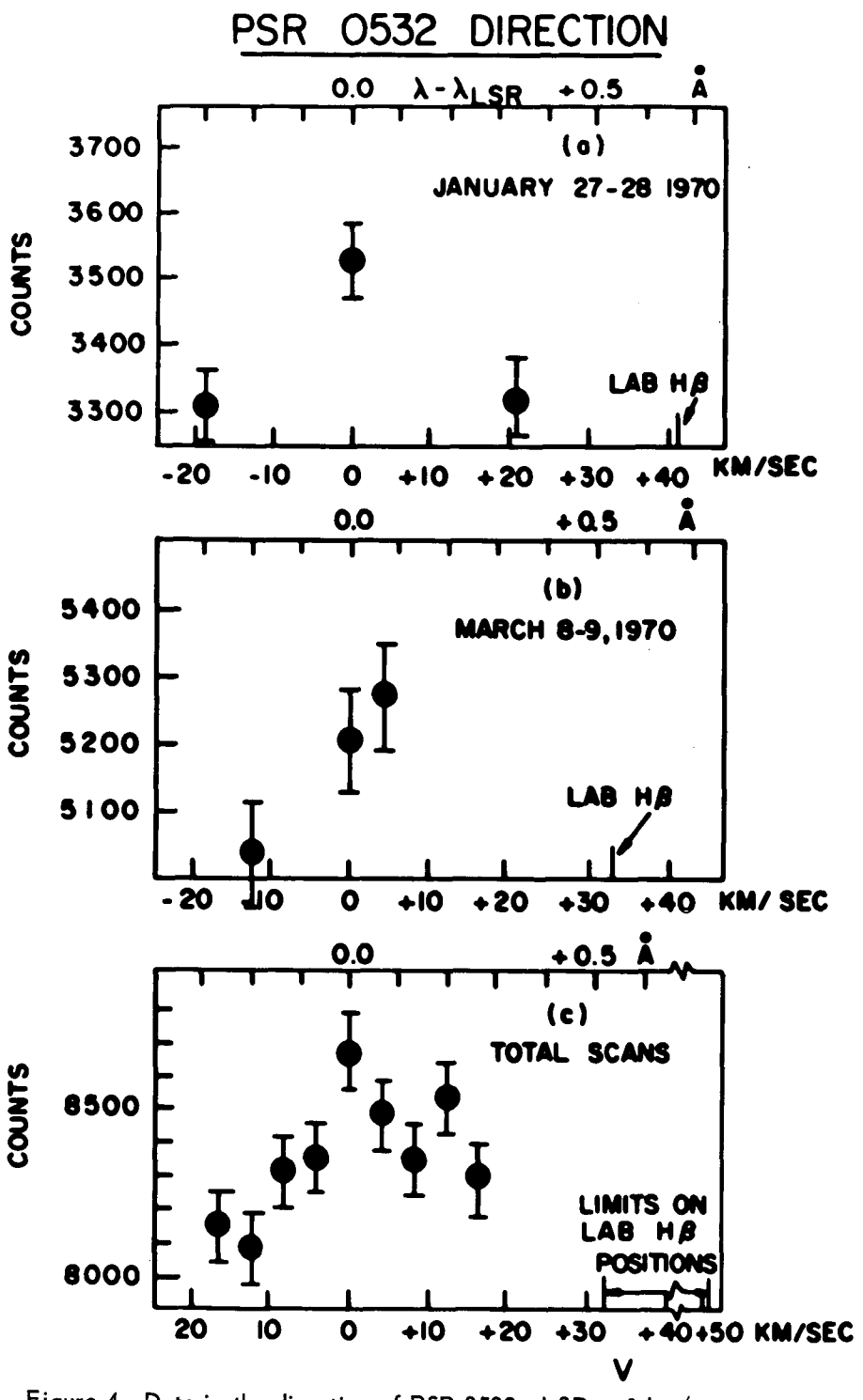

Figure 4. Data in the direction of PSR 0532. LSR at 0 km/sec.
(a) data of January 27-28, 1970; 2000 sec/point.
(b) data of March 8-9, 1970; 3000 sec/point.
(c) sum of all 62 continuous scans from November 16, 1969 through February 28, 1970; 3720 sec/interval; 0.067 Å/interval; direction of observations:
RA $= 05^h 32^m 6.4^s$
DEC $= +22^\circ 00' 05''$ 1970

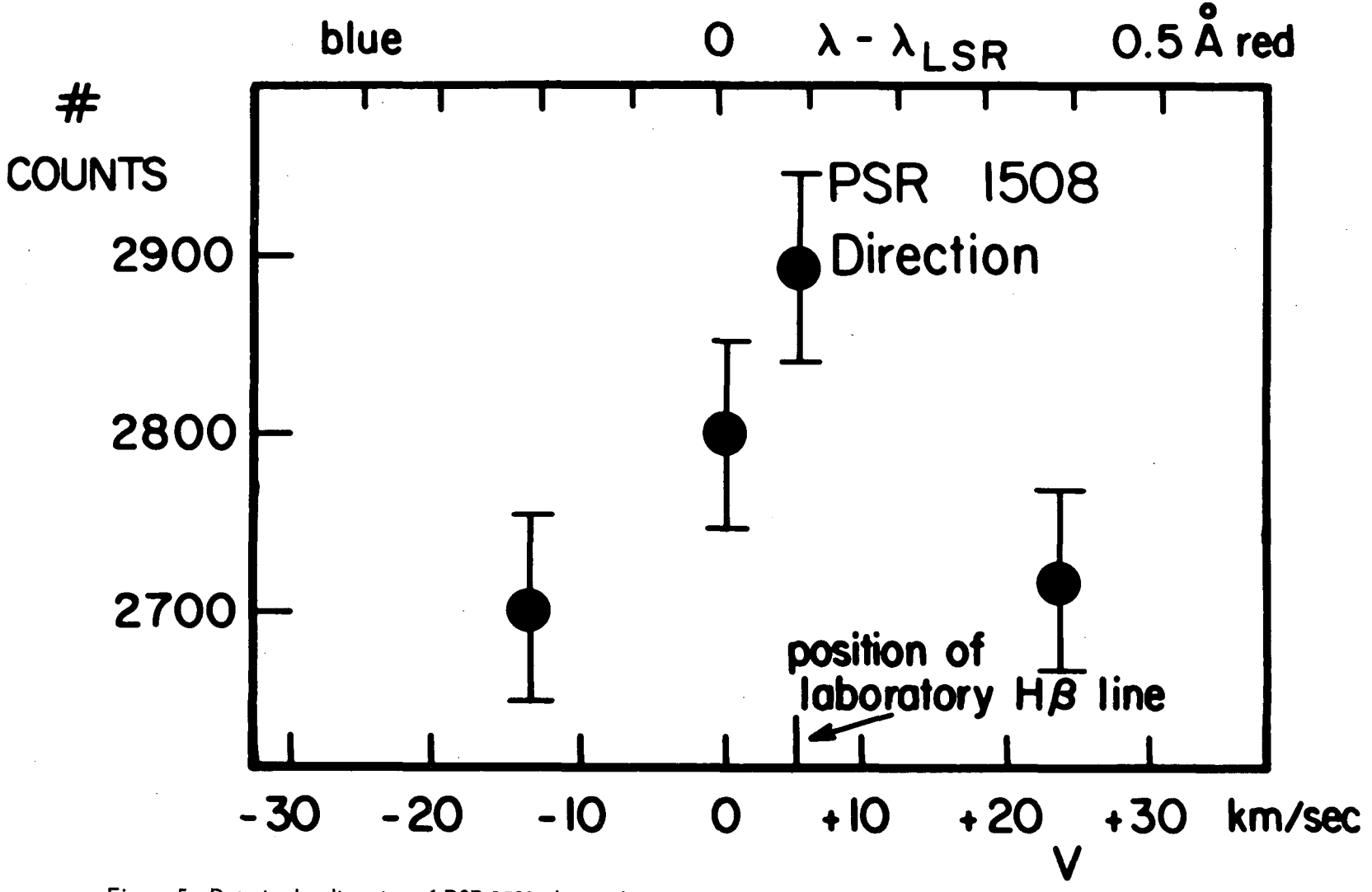

Figure 5. Data in the direction of PSR 1508 obtained May 29-30, 1970; 2700 sec/point; direction of observation:
RA = $15^h\ 08^m\ 03^s$
DEC = $+55°\ 46'\ 00''$ 1970

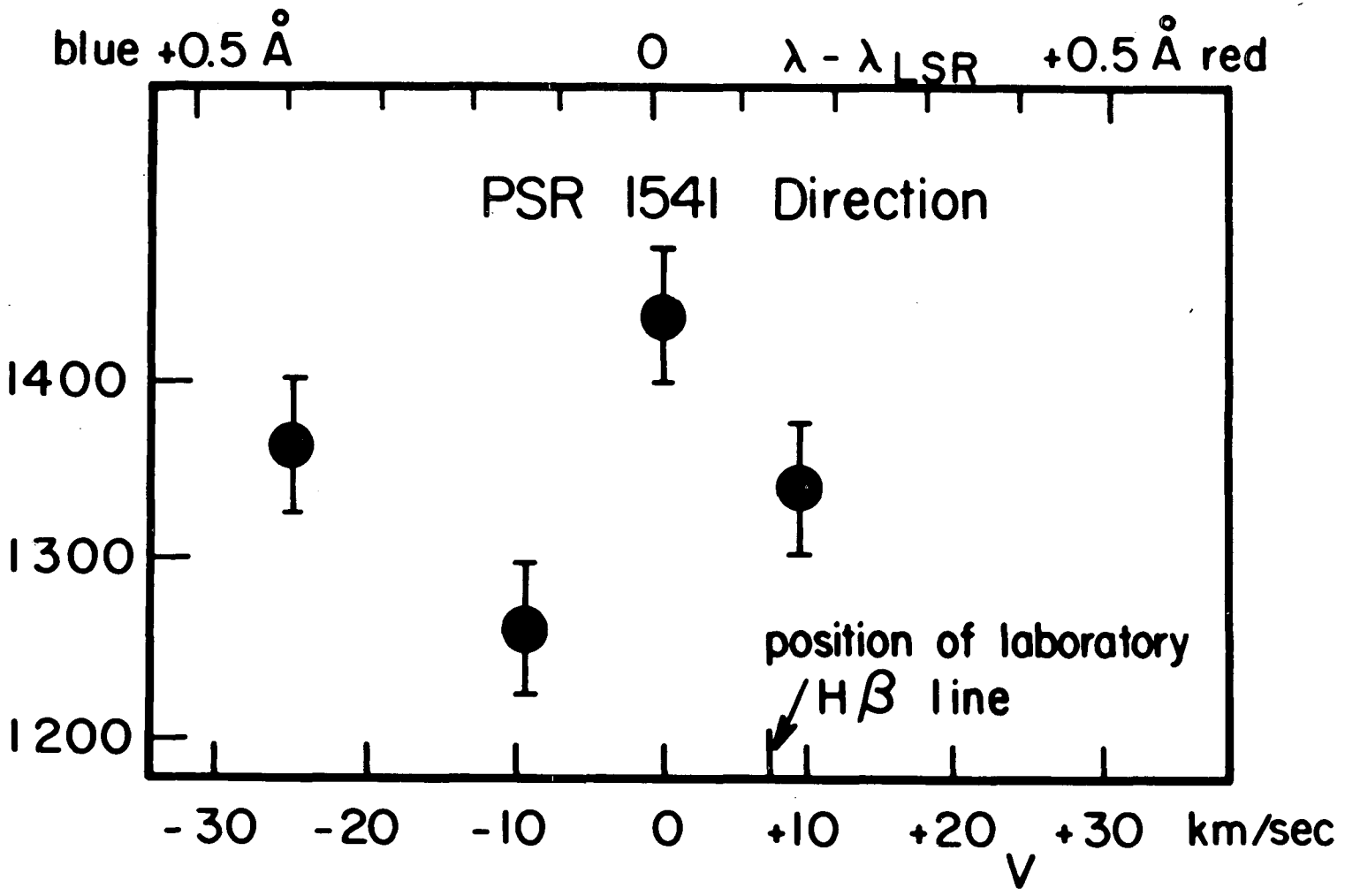

Figure 6. Data in direction of PSR 1541 obtained May 31 – June 2, 1970. 1400 sec/point;
direction of observation : RA = $15^h\ 41^m\ 35.0^s$
DEC = $+09^\circ\ 38'\ 00''$ 1970

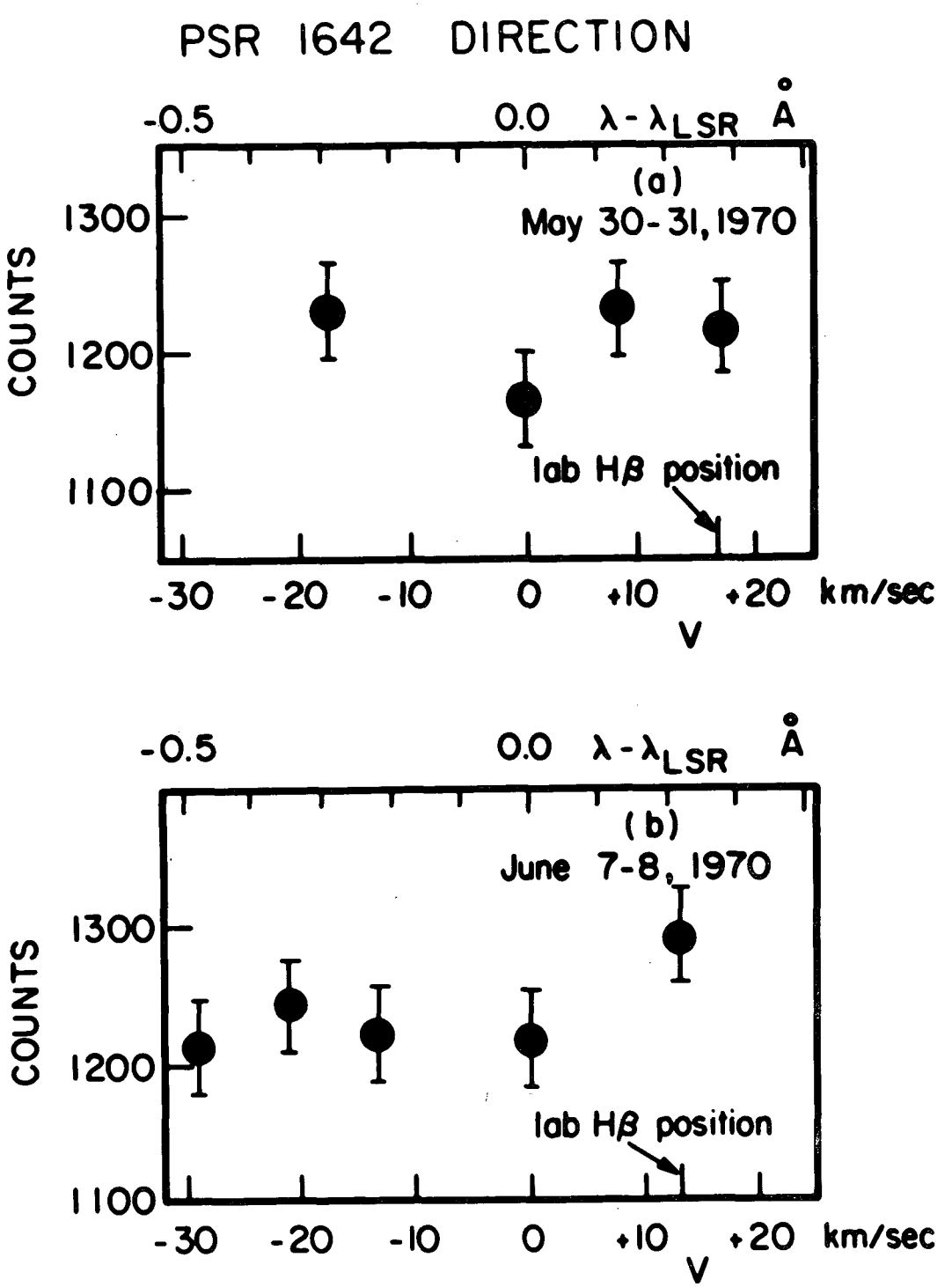

Figure 7. Data in the direction of PSR 1642.
(a) data of May 30-31, 1970; 900 sec/point
(b) data of June 7-8, 1970; 1000 sec/point

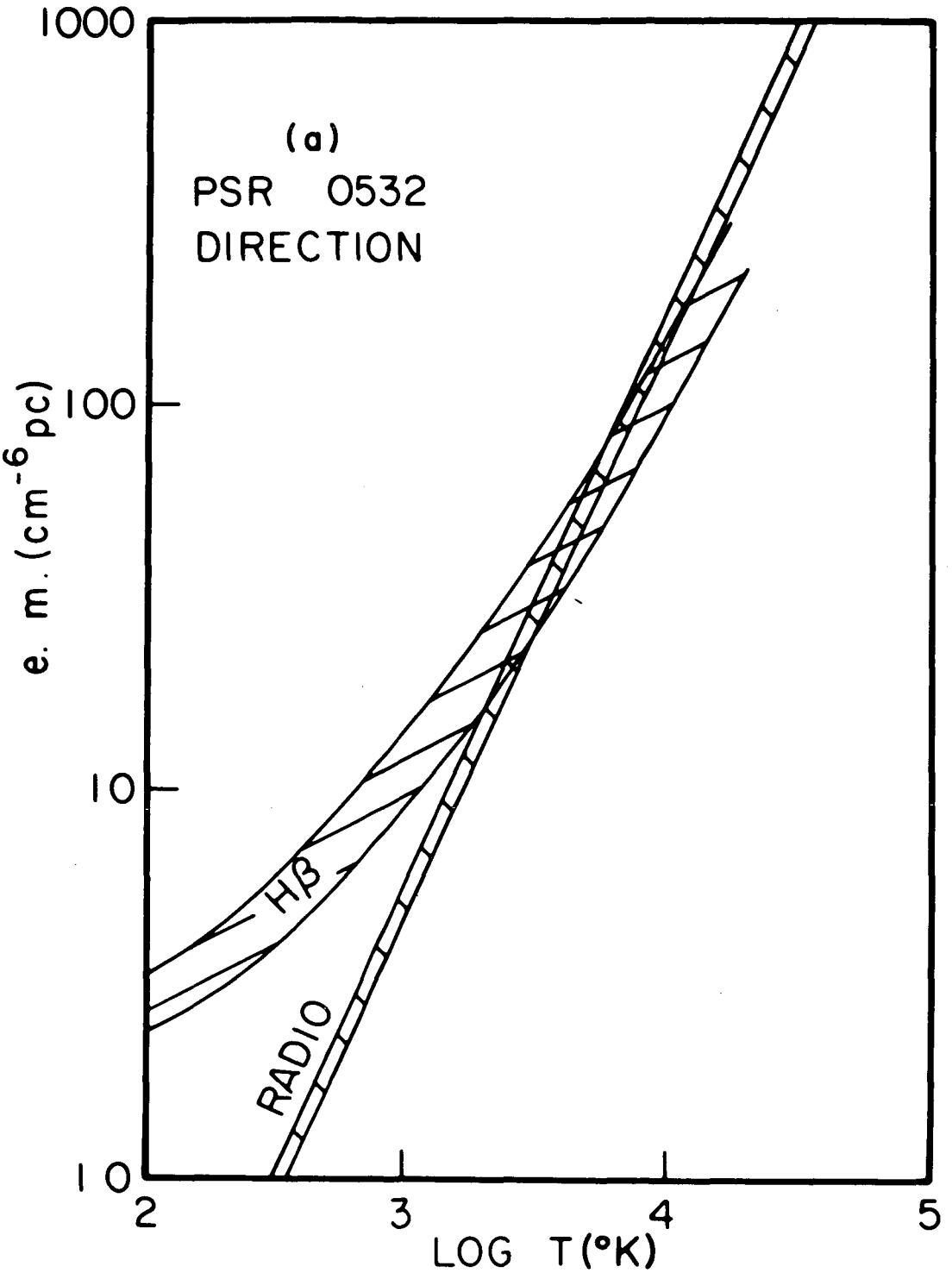

Figure 8. Comparisons of e.m. (T_e) from the radio absorption measurements of Ellis and Hamilton (1966) with e.m. (T_e) drived from the observed H-beta intensities. The cross-hatched regions represent the area bounded by ±1 standard deviation in the data. (a) direction near PSR 0532.

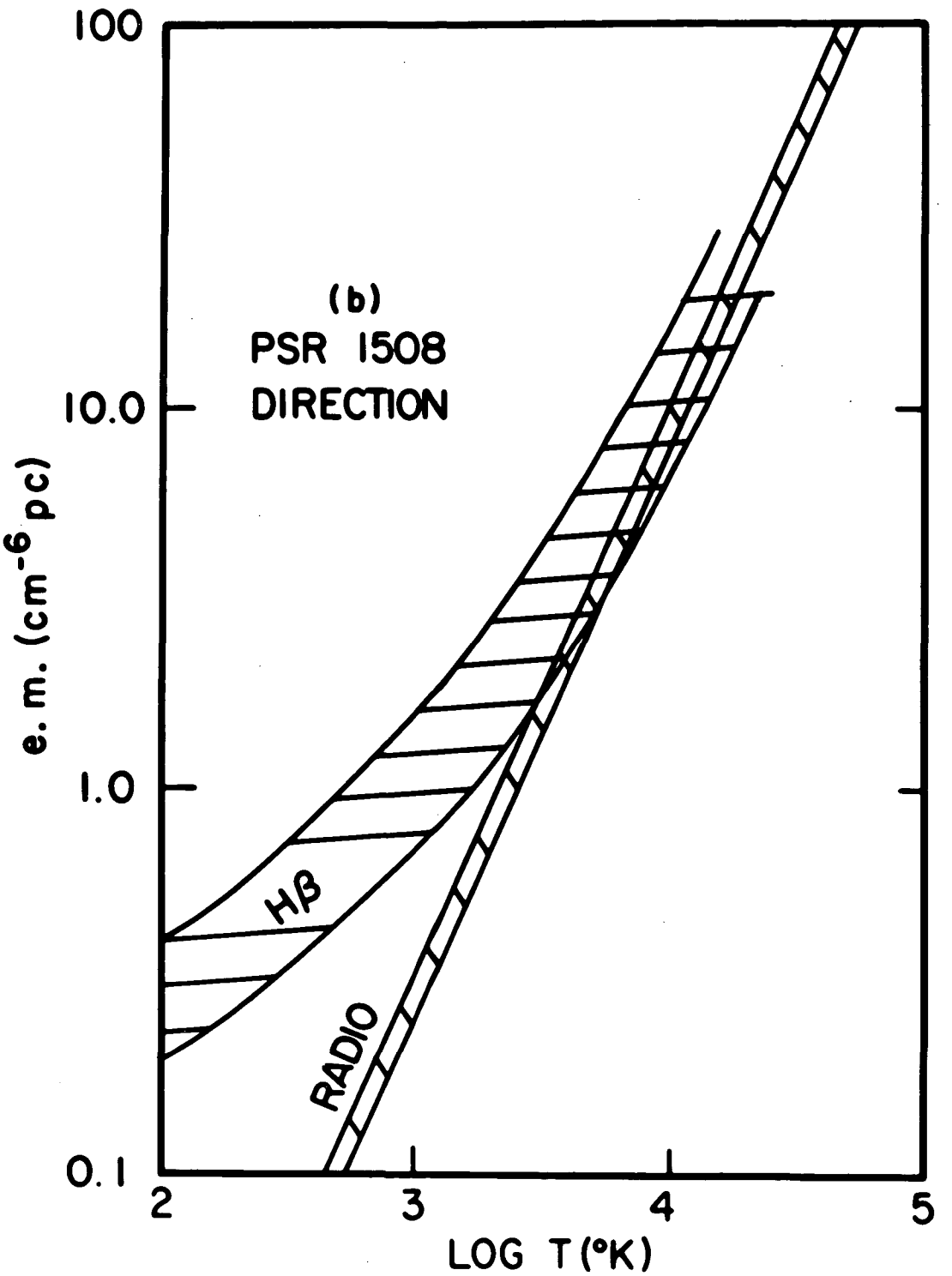

Figure 8. (b) direction near PSR 1508.

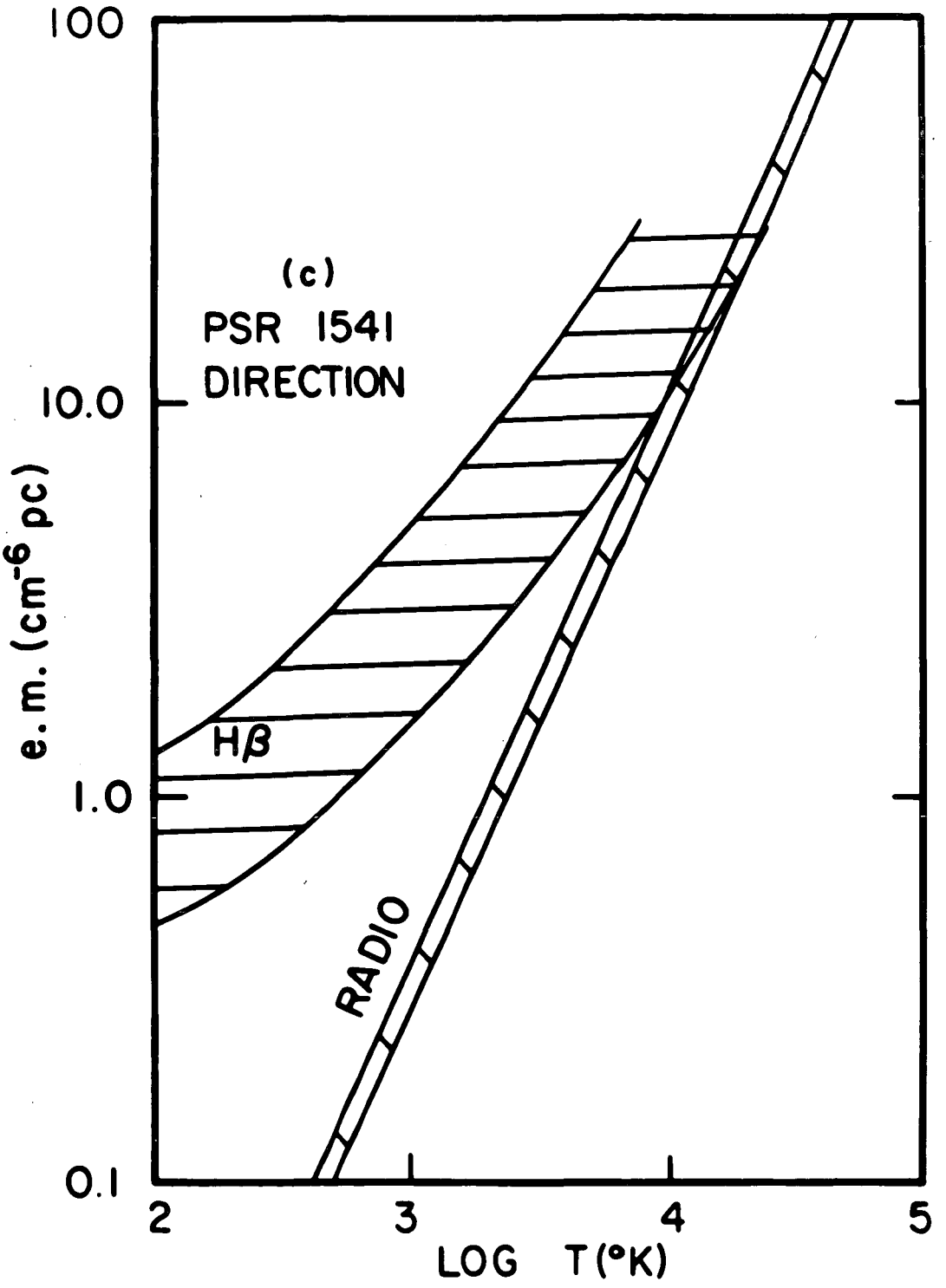

Figure 8. (c) direction near PSR 1541.

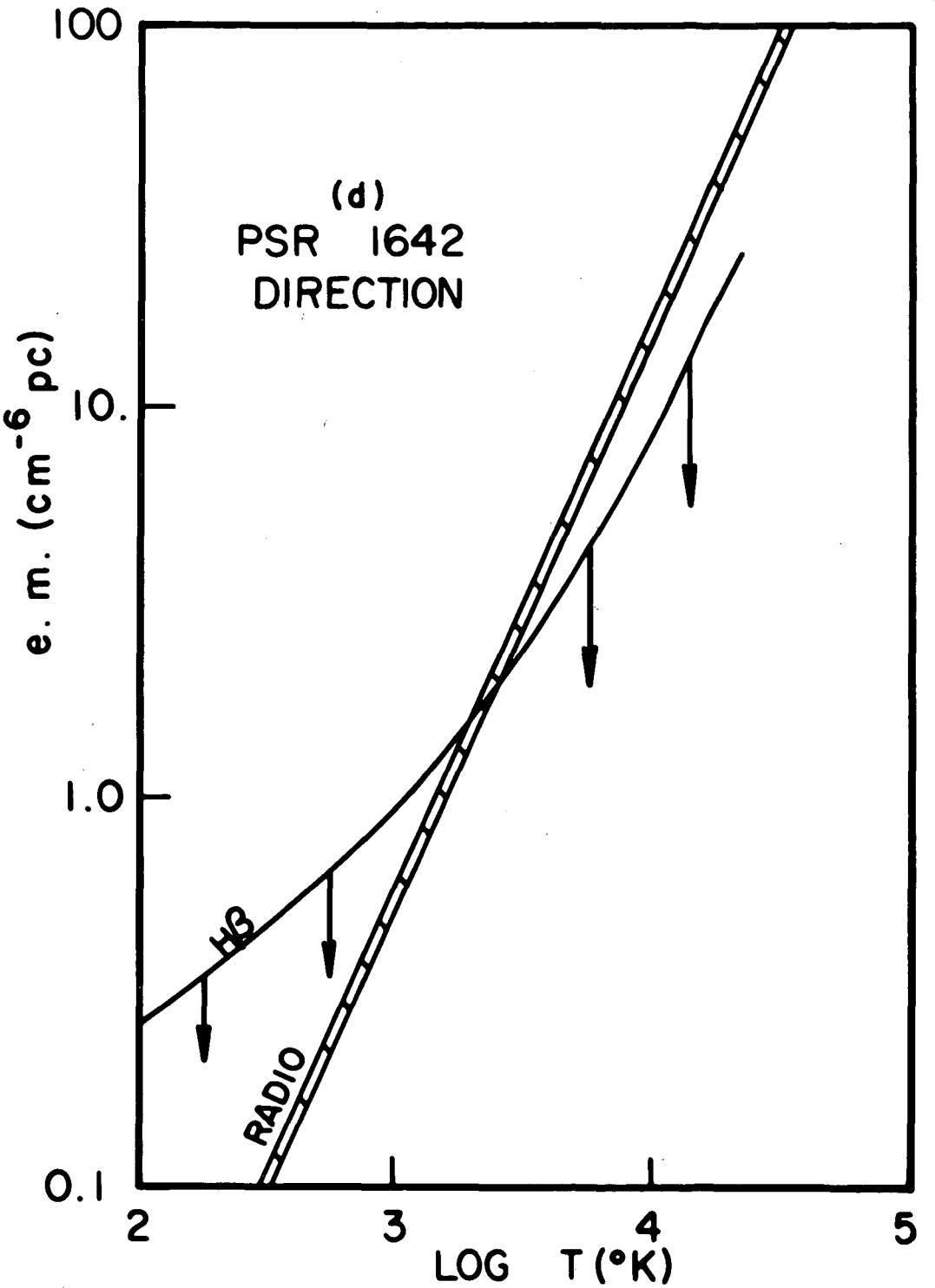

Figure 8. (d) direction near PSR 1642. The single solid line represents the upper limit to e.m. as derived from the H-beta observations assuming no extinction.